Dynamic mechanical analysis of rubber-based products in under ballast mat rail applications

Colin Bradley[1]
Faiz Musafere[2]
Josh Havin[3]
Pliteq, Inc.
131 Royal Group Crescent
Vaughan, ON, Canada, L4H 1X9

ABSTRACT

Rubber has long been a material used for vibration isolation in railroad applications due to the attractive material performance and environmental stability. In addition to the inherent sustainability benefits relative to alternatives, rebonded rubber in particular offers the opportunity for further material engineering by controlling particle size distribution, density, binder properties etc. at the manufacturing stage and has found widespread use globally in under ballast mat applications from tramway to heavy-haul/mainline track types. In this paper we explore in detail the basic vibration isolation properties of a variety of rebonded rubber-based ballast mats via dynamic mechanical analysis and connect fundamental properties such as dynamic modulus, natural frequency, degree of damping to the relevant design criteria defined in widely accepted industry standards DIN 45673-5 and the more recent EN 17282.

1. INTRODUCTION

As the importance of rail infrastructure steadily increases around the world due to the efficiency, capacity and environmental benefits relative to alternative modes of transportation. The incidence rate of sensitive acoustic adjacencies has skyrocketed.[1] In addition to the benefits to ballast preservation and track modulus control across transition zones, the ballast mat has been established as a standard solution across a broad range of scenarios requiring ever stricter vibration mitigation.[2]

In this paper we will take a high-level approach at characterizing the behavior of commercially available and prototype rubber-based ballast mats, focusing on the fundamental properties of these materials that dynamic mechanical analysis can provide. This includes deflection behavior, natural frequency, dynamic modulus, and degree of damping among other geometric properties.

At a very basic level, the benefits of incorporating acoustic isolation into design can be demonstrated using a simplified single degree of freedom lumped element model. If we consider only the vertical displacement x(t) of the system shown in Figure 1 and apply Newton's Laws of Motion we can produce Equation 1 describing the system. Where *m* is the mass being isolated, *c* is

[1]cbradley@pliteq.com
[2]fmusafere@pliteq.com
[3]jhavin@pliteq.com

the damping coefficient, k is the stiffness of the isolator, x is the vertical displacement and F is an external periodic excitation force.

$$m\,x''(t) + c\,x'(t) + k\,x(t) = F(t) \tag{1}$$

This second-order differential equation can then be solved, prompting some useful definitions, see Equations 2 and 3:

Natural Frequency (rad/s): $$2\pi\, f_n = \sqrt{\frac{k}{m}} = \omega_n \tag{2}$$

Critical Damping Ratio: $$\zeta = \frac{c}{2\,m\,\omega_n} = Loss\ Factor\ \eta/2 = \tan(\delta)\,/2 \tag{3}$$

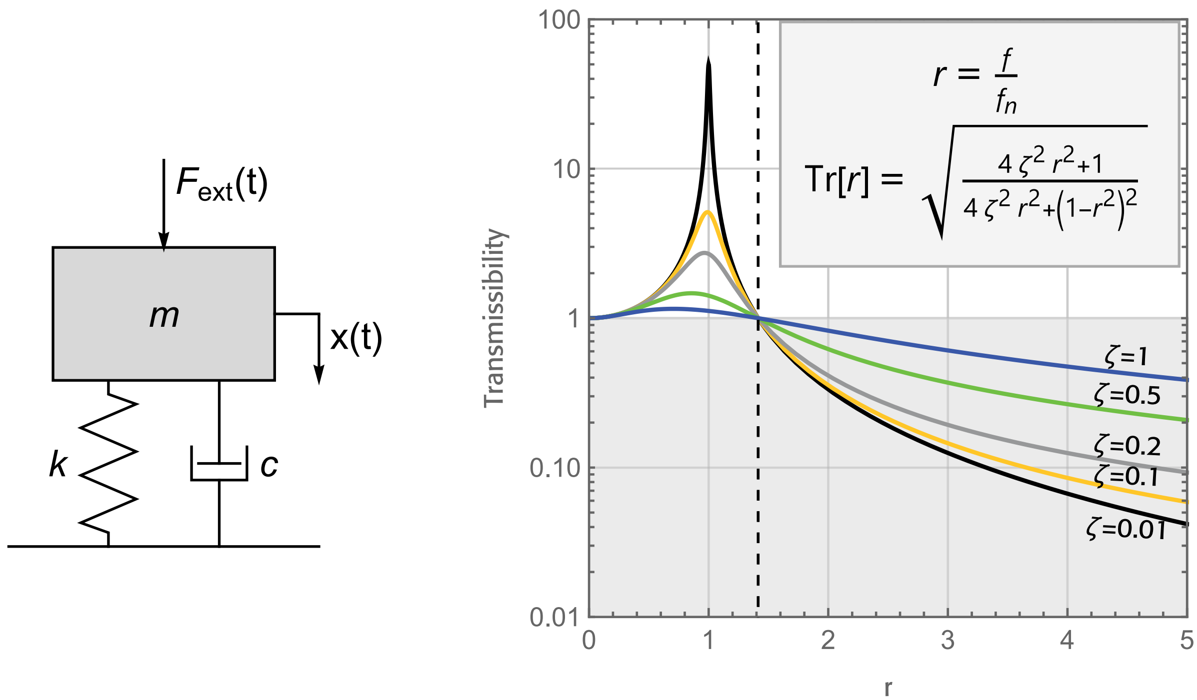

Figure 1: Single Degree of Freedom lumped element model for simple forced harmonic motion and the resulting transmissibility as a function of forcing frequency to natural frequency.

The stiffness and degree of damping for isolating materials are a function of the magnitude, frequency distribution and amplitude of the applied load. Characterization of the dynamic properties of viscoelastic materials is measured using dynamic mechanical analysis techniques as described in DIN 53513. The dynamic or complex modulus of the material can be ascertained across the relevant load range, frequency and amplitude of vibration. The complex modulus includes the increased stiffness due to viscous losses in the material.[3]

Of interest when engineering vibration isolation systems is the ratio of the force transmitted to the force input, or transmissibility. See Equation 4.

Transmissibility: $$Tr\left({}^{\omega}/_{\omega_n}\right) = \frac{F_{base}}{F_{ext}} \tag{4}$$

Transmissibility is a function of frequency. For frequencies near the natural frequency of the system, amplification will occur. For frequencies well above the natural frequency, isolation will occur. The crossover point is at $\sqrt{2}\omega_n$ for this simplified model of the vehicle-rail-ballast-ballast mat system.

The behavior of the system also depends on the degree of damping. In this context we are interested in the underdamped scenario (ζ<1). The greater the damping of the system, the less amplification will occur near the natural frequency but also the less isolation will be provided at higher frequencies.

Steel has a critical damping ratio of ζ: 0.005-0.01, while resilient materials such as rubber will have a critical damping ratio of ζ: 0.05-0.15 for example. [4]

Finally, we will explore the importance, or lack thereof, of the shape factor of these resilient materials. Here we define shape factor as the ratio of loaded area to unloaded perimeter area of the sample.

Shape Factor:
$$u = \frac{Loaded\ Area}{Unloaded\ Perimeter\ Area} \tag{5}$$

This oversimplified model of the ballast mat system will suffice for the purpose of comparing fundamental properties of the materials tested which will then be compared to the resulting dynamic and static parameters as measured by the widely accepted DIN 45673-5 and more recent EN 17282 standards relating to ballast mat performance in rail applications. [5,6]

While outside the scope of this paper, the reader is encouraged to browse [7,8,9,10] for details on how to use these measured properties to predict insertion loss performance, in-service deflection, a more sophisticated treatment of the system incorporating multi-degree of freedom analysis, a variety of mechanical models of the isolator such as Kelvin-Voight, Maxwell, Fractional Zener etc.

3. PROCEDURE AND SAMPLE PREPARATION

For this study, six crumb-rubber based materials and one mixed-cell polyethylene foam material of varying formulations and geometry will be subjected to dynamic mechanical analysis using a test frame capable of 10 kN of force up to 200 Hz. At least three samples of a given formulation type and geometry have been produced to provide statistical confidence in the results. See Table 1.

Although detailed descriptions of the formulations cannot be shared widely due to trade secret concerns, a broad range of particle size distributions, density, geometry and binder content have been selected to demonstrate the flexibility of such materials in the context of ballast mat performance.

An extended procedure based on DIN 53513 for measuring the dynamic modulus of viscoelastic materials was developed in order to explore the important fundamental dynamic properties, the parameters include:

1. Displacement amplitudes of $\pm 0.02\ mm$, $0.06\ mm$, $0.10\ mm$, $0.20\ mm$
2. Mean load range 0.025 - 0.25 MPa in steps of 0.025 MPa
3. Frequency range of less than 1 Hz, 10 Hz, 20 Hz, and 30 Hz
4. Load vs Natural Frequency (0.02 MPa - 0.20 MPa)
5. Shape Factors between $u = 0.8$ and $u = 2.6$. Repeat measurements 1 through 4.

Table 1: Sample Matrix

Sample I.D.	Shape Factor	Formulation	Base Material
A-01	2.5	Type A	Crumb Rubber
A-02	2.5	Type A	Crumb Rubber
A-03	2.5	Type A	Crumb Rubber
B-01	2.2	Type B	Crumb Rubber
B-02	2.2	Type B	Crumb Rubber
B-03	2.2	Type B	Crumb Rubber
C-01	1.4	Type C	Crumb Rubber
C-02	1.4	Type C	Crumb Rubber
C-03	1.4	Type C	Crumb Rubber
D-01	1.4	Type D	Crumb Rubber
D-02	1.4	Type D	Crumb Rubber
D-03	1.4	Type D	Crumb Rubber
E-01	2.5	Type E	Mixed-Cell Foam
F-01	2.5	Type F	Crumb Rubber
F-02	2.5	Type F	Crumb Rubber
F-03	2.5	Type F	Crumb Rubber
D-04	2.6	Type D	Crumb Rubber
D-05	2.6	Type D	Crumb Rubber
D-06	2.6	Type D	Crumb Rubber
D-07	1.4	Type D	Crumb Rubber
D-08	1.4	Type D	Crumb Rubber
D-09	1.4	Type D	Crumb Rubber
D-10	0.8	Type D	Crumb Rubber
D-11	0.8	Type D	Crumb Rubber
D-12	0.8	Type D	Crumb Rubber

4. RESULTS AND DISCUSSION

4.1. Load v Strain

The static strain due to loading up to 0.30 MPa was measured for all samples and the results are presented in Figure 2. Within the same material type the spread of the results was quite small with the exception of Type C materials which showed a moderate variance in strain of up to 10% at high loads. Below about 0.08 MPa this variance reduced to < 3%. All other materials were within a few percentage points across at least three samples, demonstrating a high degree of uniformity in strain behavior. This includes all Type D samples, which consists of the additional samples for the shape factor exploration (Type D-04 – Type D-10).

Apart from material Type E, each of these materials is rubber based, differing in formulation, density, particle size distribution only. With those parameters available, the behavior of the material can be tuned to behave in a wide variety of modes, whether it be consistent stiffness across a wide load range like Type B, or small, moderate or significant strain as the load increases.

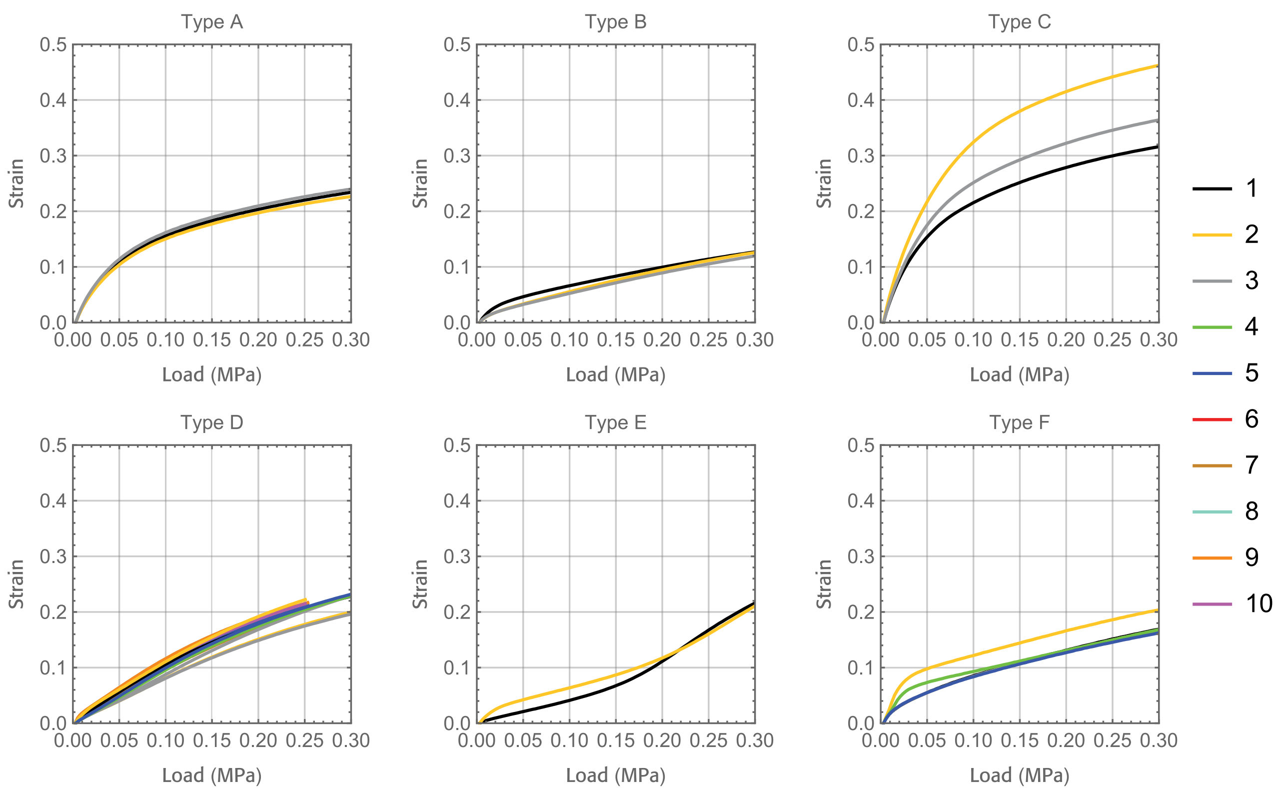

Figure 2: Static loading vs Strain (L/L_0) for all materials.

4.2. Load v Natural Frequency

The natural frequency vs load as measured by frequency sweep analysis is shown in Figure 3. Again, a wide variety of behavior is on display, with natural frequencies ranging from the mid-20s to 10 Hz at higher loads. Some materials such as Type A, C and to some extent D show consistent natural frequencies across a wide load range, while others require higher loads before the natural frequency drops to the minimum level.

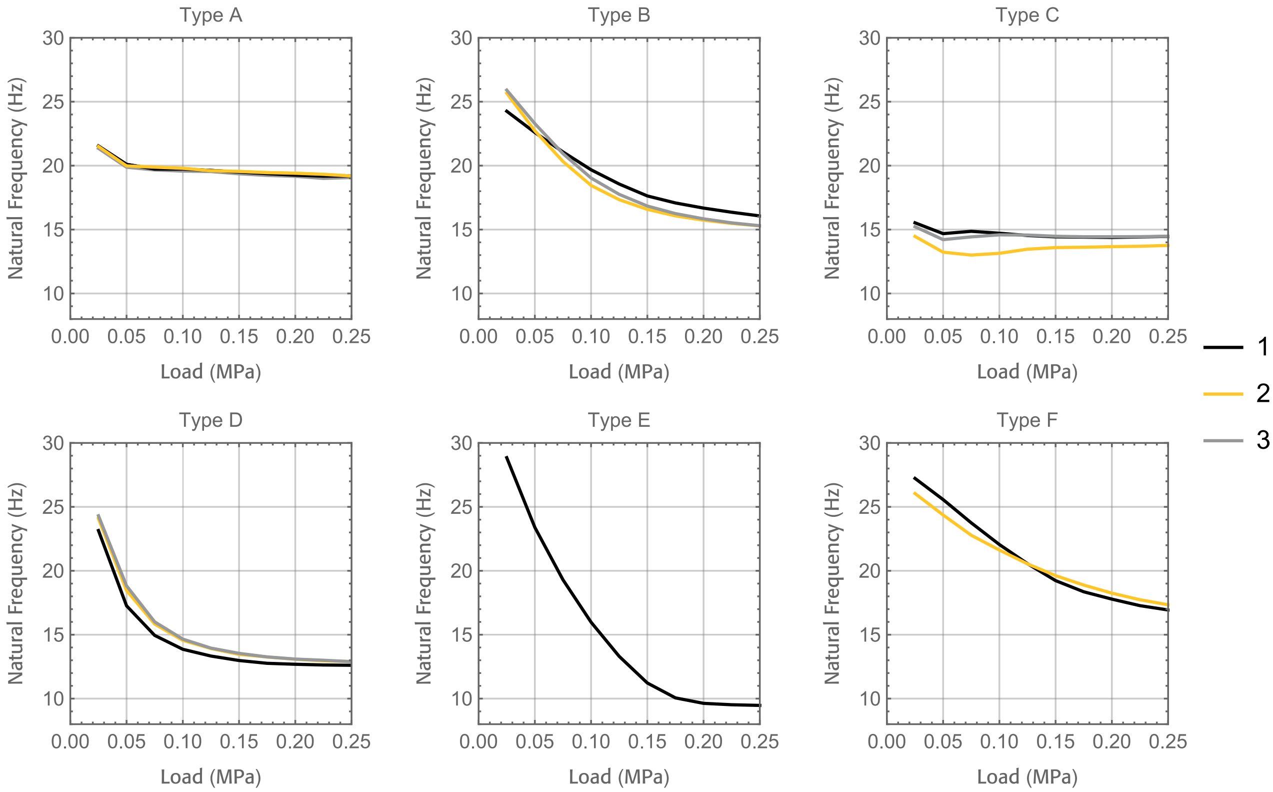

Figure 3: Natural Frequency vs Load with an amplitude of oscillation of 1 mm p-p.

4.3. Effect of Oscillation Amplitude and Shape Factor on Natural Frequency

The impact of oscillation amplitude and shape factor was explored in depth for the Type D material, the results of which are shown in Figure 4. The overall curve shape remains constant through the range of amplitude and shape factors tested here. The impact of shape factor is negligible between the largest samples and smallest samples (top to bottom in Figure 4). The natural frequency remains within 1 Hz as the shape factor is reduced by over 100%.

The p-p amplitude of oscillation causes the natural frequency to drop by several Hz as the amplitude increases from 0.2 mm to 2.0 mm (left to right in Figure 4). As the amplitude of oscillation increases the complex component of the modulus plays a larger role.

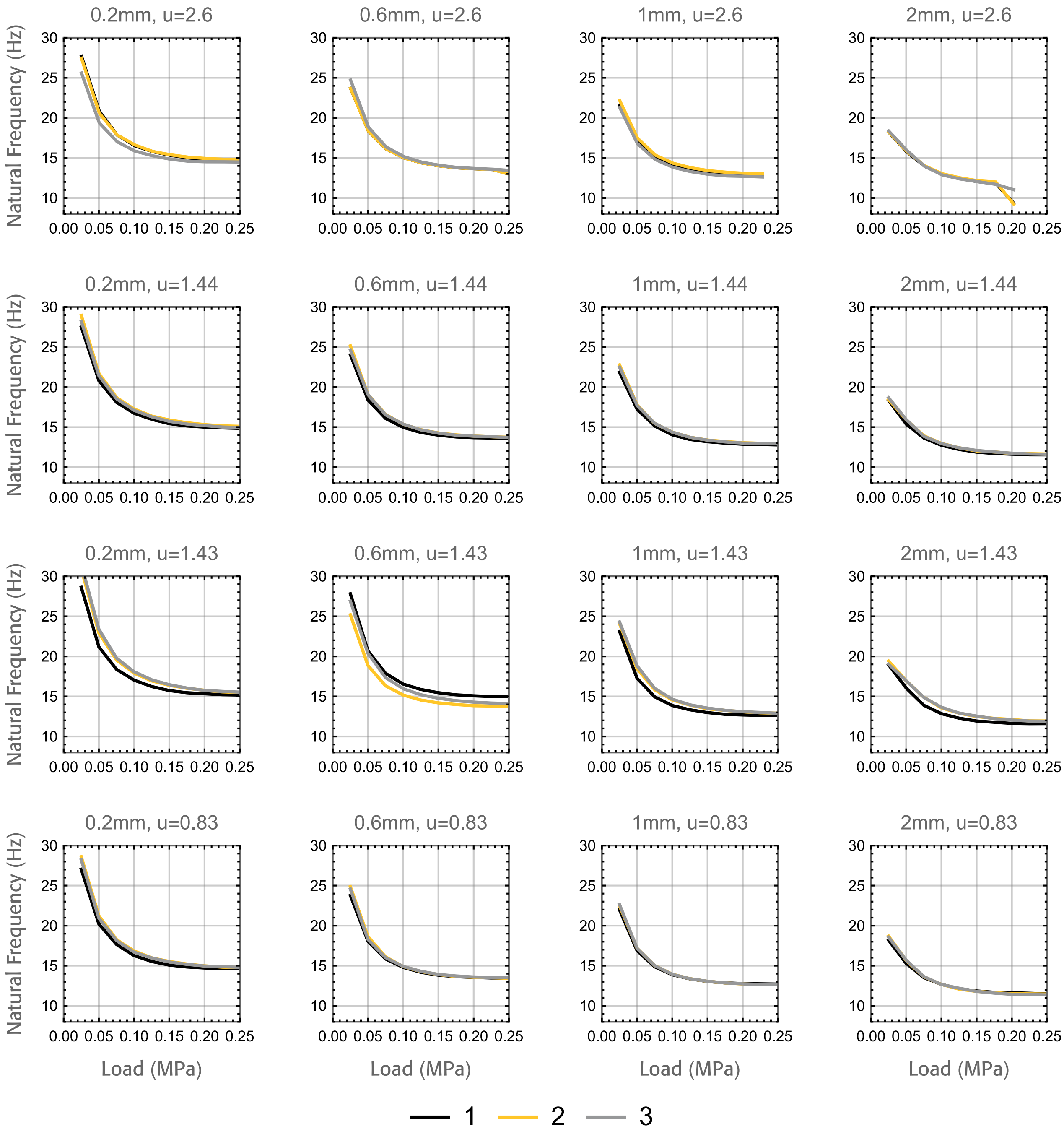

Figure 5: Impact of shape factor and amplitude of oscillation on Type D samples. From left to right increasing p-p amplitude from 0.2 mm to 2.0 mm and from top to bottom decreasing shape factor from 2.6 to 0.83.

4.4. Dynamic Modulus, Frequency, and Load

The dynamic modulus of each material was measured in accordance with DIN 53513 at pseudo steady-state, 10 Hz, 20 Hz, and 30 Hz. See Figure 6. The rubber-based products demonstrate consistent behavior with varying rates of stiffening as the load increases from 0 to 0.25 MPa. The mixed-cell foam material, Type E, is the outlier with a dynamic modulus that oscillates around an average value. In every case the increasing the forcing frequency from less than 1 Hz to 30 Hz increases the modulus by 5 to 15% as the viscous forces begin to contribute significantly to the overall stiffness.

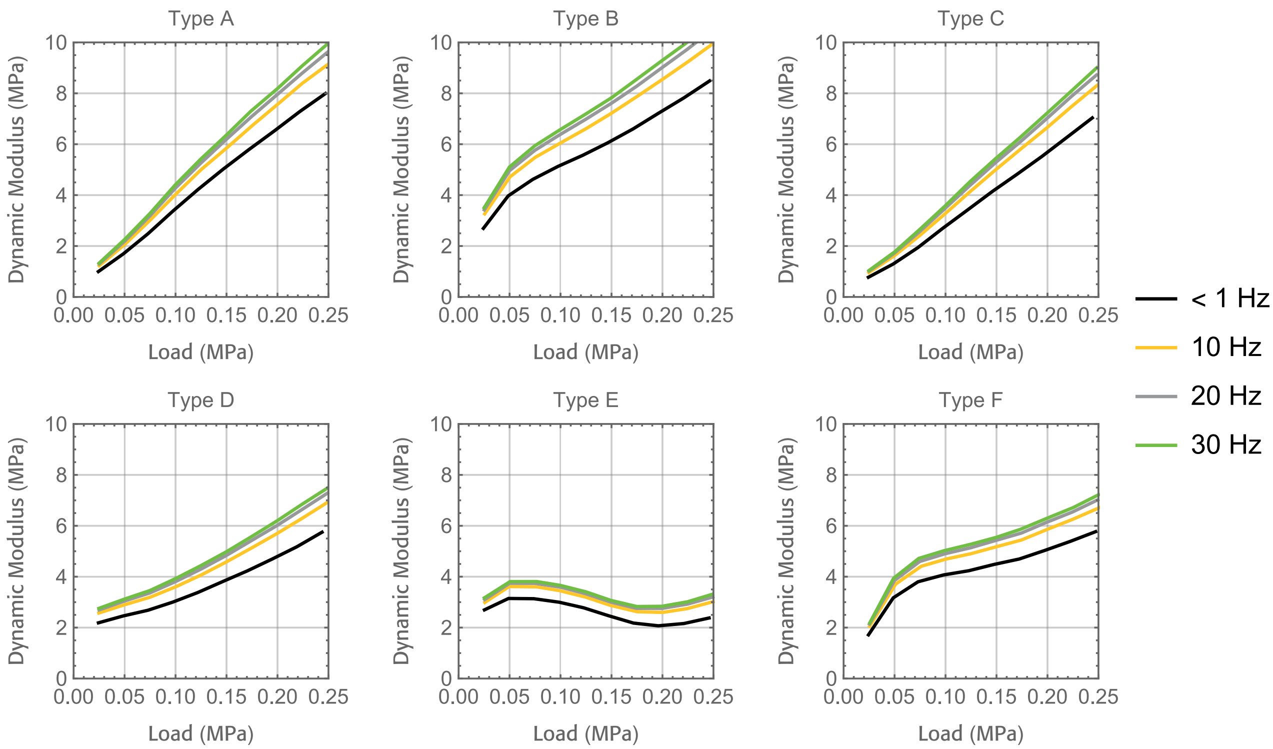

Figure 6: Measured Dynamic Modulus for each material type according to DIN 53513, oscillation amplitude of 0.2 mm p-p, shape factor >1.4.

5. CONCLUSIONS

In this work, we have taken the often over-simplified material of rubber crumb and demonstrated the broad range of relevant acoustical properties possible by controlling such manufacturing parameters as particle size distribution, density, geometry and binder content. Comparing it to other such engineered materials like mixed-cell polyethylene foam.

By modifying and extending the procedure for the measurement of viscoelastic properties according to DIN 53513. The effect of oscillation amplitude, shape factor, frequency and loading in the context of ballast mat systems was explored. In all cases the materials remained well-behaved and consistent, while the effect of shape factor was shown to be minimal and the correlation between oscillation amplitude yielded lower natural frequencies with increased amplitude.

Future work will include the correlation between these fundamental material properties and the ballast mat specific performance based on established industry standards.

6. REFERENCES

1. Hanson, C. E., Towers, D. A., & Meister, L. D. (2006). Transit Noise and Vibration Impact Assessment -FTA Federal Transit Administration. Transit Noise and Vibration Impact Assessment, May, 1–261.
2. Hanson, C. E., & Singleton, H. L. J. (2006). Performance of ballast mats on passenger railroads: Measurement vs. projections. *Journal of Sound and Vibration*, *293*, 873–877.
3. M. Long, “Vibration and Vibration Isolation” Chap. 11 in Architectural Acoustics Elsevier Academic Press, New York, 2006.

4. *DIN 53513 - Determination of Viscoelastic Properties of Elastomers.pdf*. (n.d.).
5. Schwingungen, M., Elemente, E., Teil, S., & Obersetzung, U. E. (2010). *DIN 45673-5 Mechanical Vibration - RESILIENT ELEMENTS USED IN RAILWAY TRACKS*. *August*, 1–19.
6. EN 17282:2020-10 Railway Applications—Infrastructure—Under Ballast Mats; CEN: Brussels, Belgium, 2020.
7. Lima, A. O., Dersch, M. S., Qian, Y., Tutumluer, E., & Edwards, J. R. (2017). Laboratory evaluation of under-ballast mat effectiveness to mitigate differential movement problem in railway transition zones. *Bearing Capacity of Roads, Railways and Airfields - Proceedings of the 10th International Conference on the Bearing Capacity of Roads, Railways and Airfields, BCRRA 2017*, 1969–1975. https://doi.org/10.1201/9781315100333-260
8. Kraśkiewicz, C., Zbiciak, A., Wasilewski, K., & Sabouni-Zawadzka, A. Al. (2021). Laboratory tests and analyses of the level of vibration suppression of prototype under ballast mats (Ubm) in the ballasted track systems. *Materials*, *14*(2), 1–18. https://doi.org/10.3390/ma14020313
9. Li, Z. (2019). Vibration transmissibility of two-DOF vibrating systems. *INTER-NOISE 2019 MADRID - 48th International Congress and Exhibition on Noise Control Engineering*, *1*.
10. Wettschureck, R.G.; Heim, M.; Mühlbachler, S. Reduction of structure-borne noise emissions from above-ground railway lines by means of ballast mats. In Proceedings of the INTER-NOISE and NOISE-CON Congress and Conference, Budapest, Hungary, 25–27 August 1997; Volume 97, pp. 577–580.